Proc. Estonian Acad. Sci. Phys. Math., 1990, 39, N 3, 268—275
https://doi.org/10.3176/phys.math.1990.3.11

УДК 535.55

Hillar ABEN, Siim IDNURM and Alfred PURO

INTEGRATED PHOTOELASTICITY IN CASE OF WEAK BIREFRINGENCE

1. Introduction

In integrated photoelasticity stresses in three-dimensional models are determined using optical data obtained when polarized light passes through the whole model in a transmission polariscope. In this respect integrated photoelasticity may be interpreted as optical tomography of the stress field. However, while classical tomography is restricted to the determination of scalar fields, in integrated photoelasticity one has to determine a tensor field.

The optical phenomena in integrated photoelasticity are very complicated due to the rotation of principal axes along the light rays. However, if birefringence of model is weak, the measurements are similar to those with two-dimensional models and simple integral relationships between the experimental data and the stress components are valid. This permits to elaborate methods for nondestructive determination of stress in a three-dimensional transparent specimen.

2. Integrated photoelasticity as optical tomography of the stress field

In integrated photoelasticity [1] we immerge the three-dimensional model into an immersion bath and pass a beam of polarized light through the model (Fig. 1). Transformation of the polarization of light is measured for many light rays. In certain cases the stress distribution can be determined using this integrated optical information.

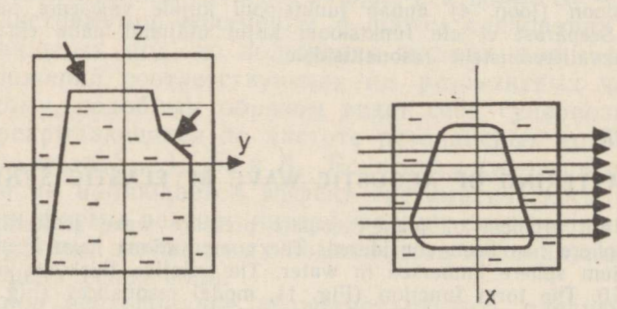

Fig. 1. Experimental set-up in integrated photoelasticity.

Since the determination of stresses is usually carried out by sections, integrated photoelasticity can be considered to be a kind of optical tomography [2]. However, this tomography has several important specific features [3, 4].

It is essential to point out that classical tomography is scalar field tomography. It means that every point of the field is characterized by a single number. It may be the extinction coefficient of X-rays, scalar acoustical refraction index, etc. Stress field, on the contrary, is a tensor field, i. e. every point of the field is characterized by a symmetric second-rank tensor which has six independent components.

Other particular features of tensor field tomography are the following.

The influence of a point of a scalar field on the passing radiation does not depend on the direction of the latter, since a scalar is geometrically represented by a sphere. The influence of a point of a tensor field depends on the direction of the passing radiation since a tensor is geometrically represented by an ellipsoid.

In scalar field tomography nonpolarized radiation is usually used. In tensor field tomography polarized radiation has to be used since it is more informative.

Scalar field tomography is based on line integrals of the field. In the general case of integrated photoelasticity [1] one has to determine the characteristic directions and the characteristic phase retardation which are related to the stress components in a nonlinear way. Line integrals of the stress components can be measured only in exceptional cases, as will be shown below.

Since a scalar field is uniquely determined by the Radon inversion [2], there is no need for *a priori* information about the field. In the case of a tensor field the number of unknowns is much larger and there obviously is a need for *a priori* information. In case of integrated photoelasticity, one has such information in the form of equations of equilibrium and compatibility, and macrostatic and boundary conditions [1, 3, 4].

3. The case of weak birefringence

As already mentioned, in the general case measurements in integrated photoelasticity give nonlinear relationships between the experimental data and the stress components [1]. Therefore, to determine the stress distribution using experimental data is very complicated.

However, if the birefringence is weak, the optical measurements can be simplified. It has been shown [5] that in the latter case a three-dimensional photoelastic model can be investigated in a usual transmission polariscope as if it were a two-dimensional model.

It means that it is possible to determine the parameter of the isoclinic ψ and the optical path difference Δ on every ray. They are related to components of the stress tensor on the ray by simple integral relationships [5]

$$\Delta \cos 2\psi = C \int (\sigma_z - \sigma_x)\, dy, \tag{1}$$

$$\Delta \sin 2\psi = 2C \int \tau_{zx}\, dy, \tag{2}$$

where C is the photoelastic constant and σ_x, σ_z and τ_{zx} are components of the stress tensor in the plane perpendicular to the light ray y.

Using numerical experiments it has been shown [5] that relationships (1) and (2) are valid if Δ is less than approximately $1/4\,\lambda$ (λ — wavelength) and the angle of rotation of the principal directions does not exceed $\pi/6$. In case of axial symmetry, Δ should be less than approximately $3/4\,\lambda$.

Thus, in case of weak birefringence, the measurements in integrated photoelasticity are similar to those in two-dimensional photoelasticity and one may use simple integral relationships (1) and (2).

Let us mention that Eqs. (1) and (2) have been used earlier by several authors [6, 7]. However, in these papers the domain of applicability of Eqs. (1) and (2) has not been considered.

4. The axisymmetric state of stress

An algorithm of integrated photoelasticity for the axisymmetric problem, using Eqs. (1) and (2), was first published by Doyle and Danyluk [7]. Here we present a somewhat different algorithm in order to underline the way equations of the theory of elasticity can be used in integrated photoelasticity.

Let us express the stress components in a section of the model in cylindrical coordinates as follows:

$$\sigma_r = \sum_{k=0}^{m} a_{2k}\varrho^{2k}, \tag{3}$$

$$\sigma_\theta = \sum_{k=0}^{m} b_{2k}\varrho^{2k}, \tag{4}$$

$$\sigma_z = \sum_{k=0}^{m} c_{2k}\varrho^{2k}, \tag{5}$$

$$\tau_{zr} = \sum_{k=1}^{m} d_{2k-1}\varrho^{2k-1}, \tag{6}$$

where (Fig. 2)

$$\varrho = r/R, \tag{7}$$

a_{2k}, b_{2k}, c_{2k} and d_{2k-1} are coefficients to be determined, and R is the radius of the section. At a distance Δz of the main section we take an auxiliary section (Fig. 2) which has the radius R' and where we denote the stress coefficients by a prime: a'_{2k}, b'_{2k}, c'_{2k}, d'_{2k-1} -

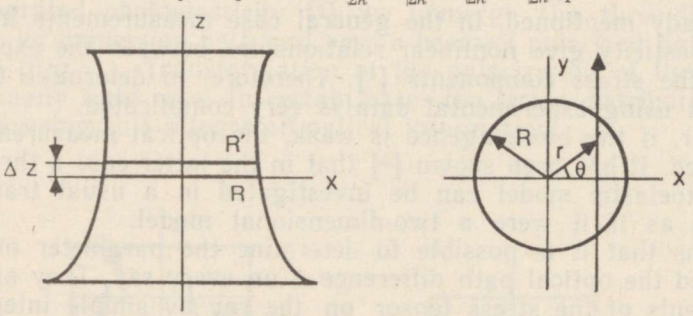

Fig. 2. Investigation of an axisymmetric state of stress.

Since on the z-axis we have $\sigma_r = \sigma_\theta$, we may write

$$b_0 = b_0. \tag{8}$$

If the external axial load P_z is known, we have

$$\int_0^{2\pi}\int_0^1 \sigma_z \varrho \, d\varrho \, d\theta = \frac{P_z}{\pi} = \sigma''_z. \tag{9}$$

Introducing expansion (5) into Eq. (9), we obtain

$$\sum_{k=0}^{m} c_{2k} \frac{1}{k+1} = \sigma''_z. \tag{10}$$

Additional relationships for the unknown coefficients may be obtained using boundary conditions.

We have to determine four functions of the dimensionless radius ϱ: σ_r, σ_θ, σ_z and τ_{zr}. However, on every light ray we may measure only two values: ψ and Δ. Consequently, we do not have sufficient information for determining the stresses directly from experimental data. To decrease the number of independent coefficients, we have to use the equations of the theory of elasticity.

If expansions (3) to (6) are introduced into the compatibility equation

$$\frac{\partial}{\partial \varrho}\left[\sigma_\theta - \mu(\sigma_r+\sigma_z)\right] - (1+\mu)\frac{\sigma_r-\sigma_\theta}{\varrho}=0, \tag{11}$$

where μ is the Poisson ratio, and into the equilibrium equation

$$\frac{\partial \sigma_r}{\partial \varrho}+\frac{\sigma_r-\sigma_\theta}{\varrho}+\frac{\partial \tau_{zr}}{\partial z}=0, \tag{12}$$

we obtain after some transformations

$$a_{2k}=\frac{2k\mu}{(2k+1)^2-1}c_{2k}-\frac{2k+1+\mu}{(2k+1)^2-1}d''_{2k-1}, \tag{13}$$

$$b_{2k}=\frac{2k\mu(k+1)}{(2k+1)^2-1}c_{2k}-\frac{1+(2k+1)\mu}{(2k+1)^2-1}d''_{2k-1}, \tag{14}$$

where

$$d''_{2k-1}=\frac{1}{\Delta\delta}\left[d'_{2k-1}\left(\frac{R}{R'}\right)^{2k-1}-d_{2k-1}\right], \tag{15}$$

$$\Delta\delta=\frac{2\Delta z}{R+R'}. \tag{16}$$

According to Fig. 2, the following relationships are valid

$$\sigma_x=\sigma_r\cos^2\theta+\sigma_\theta\sin^2\theta, \tag{17}$$

$$\tau_{zx}=\tau_{zr}\cos\theta. \tag{18}$$

Introducing Eqs. (6) and (18) into (2) reveals

$$\frac{\Delta\sin 2\psi}{4CR}=\sum_{k=1}^{m} d_{2k-1}T_{2k-1}, \tag{19}$$

where

$$T_{2k-1}=\int_0^{\sqrt{1-x_1^2}}\varrho^{2k-1}\cos\theta\,d\eta=x_1G_{2k-2}, \tag{20}$$

$$G_0=\sqrt{1-x_1^2},\quad G_{2k}=\frac{1}{2k+1}G_0+\frac{1}{2k+1}x_1^2G_{2k-2}, \tag{21}$$

$$x_1=\frac{x}{R},\qquad \eta=\frac{y}{R}. \tag{22}$$

If ψ and Δ are measured on many light rays, Eq. (19) reveals a system of linear algebraic equations for the determination of the coefficients d_{2k-1}.

For the determination of the coefficients a_0-c_0 and c_{2k}, using Eq. (1), we obtain the following system of equations

$$\frac{\Delta \cos 2\psi}{2CR} + \sum_{k=1}^{m} d''_{2k-1}(K_4 H_{2k} + K_2 F_{2k}) =$$

$$= (a_0 - c_0) G_0 + \sum_{k=1}^{m} c_{2k}(K_1 F_{2k} + K_3 H_{2k} - G_{2k}), \qquad (23)$$

where K_i are certain functions of k and H_{2k}, E_{2k} are described in [4].

Boundary or macrostatic equilibrium conditions permit to separately determine a_0 and c_0. The coefficients a_{2k} and b_{2k} can be calculated from Eqs. (13) and (14). Thus, all the stresses can be determined.

As an example, in Fig. 3 stress distribution in a grooved cylindrical rod is shown.

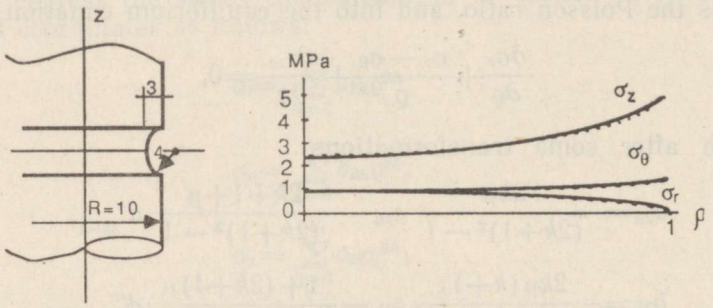

Fig. 3. Stress distribution in a grooved cylindrical rod: unbroken line — Neuber's theoretical solution [8], broken line — integrated photoelasticity (with 6 terms in the polynomials (3) to (6)).

In case of the residual stresses we cannot use the compatibility equation. However, it is possible to determine the distribution of the shear stress τ_{zr} using Eq. (19). It is also possible to determine the distribution of σ_z. For that, let us consider equilibrium condition for direction x of a three-dimensional segment ABC cut out from a body of revolution (Fig. 4).

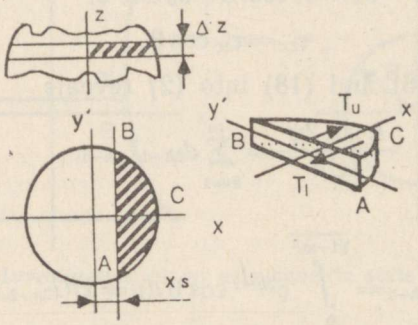

Fig. 4. Explanation of the equilibrium condition of a three-dimensional segment.

Shear force in the direction of x at the upper surface of the segment T_u can be expressed as

$$T_u = \int_{x_s}^{R'} \left(\int \tau'_{zx} \, dy' \right) dx, \qquad (24)$$

and at the lower surface as

$$T_l = \int_{x_s}^{R} \left(\int \tau_{zx} \, dy' \right) dx, \qquad (25)$$

Let us use the following notations for experimental data for the lower surface of the segment

$$V_1=\Delta\cos 2\psi=C\int(\sigma_z-\sigma_x)\,dy', \tag{26}$$

$$V_2=\Delta\sin 2\psi=C\int\tau_{zx}\,dy'. \tag{27}$$

We denote the same values for the upper surface of the segment by V_1' and V_2'.

Condition of equilibrium of the segment for direction x reveals

$$\Delta z\int_A^B\sigma_x\,dy'=T_u-T_l=\frac{1}{2C}\int_{x_s}^{R'}V_2'\,dx-\frac{1}{2C}\int_{x_s}^{R}V_2\,dx \tag{28}$$

and, taking into account Eq. (26),

$$\int_A^B\sigma_z\,dy'=\frac{1}{2C\Delta z}\left(\int_{x_s}^{R'}V_2'\,dx-\int_{x_s}^{R}V_2\,dx\right)-\frac{V_1}{C}. \tag{29}$$

Thus, integral of σ_z can be expressed through the experimental data obtained for two neighbouring sections. Knowing integrals of σ_z, the distribution of the latter is determined using the methods of the scalar field tomography.

As an example, Fig. 5 shows the distribution of axial stress σ_z in a section of a Soviet champagne bottle before and after opening.

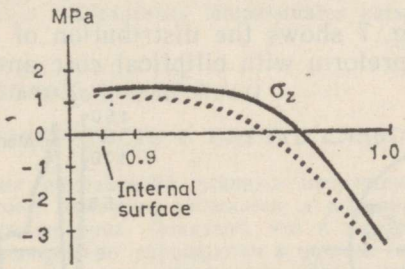

Fig. 5. Distribution of axial stress σ_z in a Soviet champagne bottle before (unbroken line) and after (broken line) opening.

5. The general three-dimensional state of stress

Let us consider an investigation of stresses in a three-dimensional body of arbitrary form. Passing light through the body in section $z=$ $=$const measurements on every ray y' (Fig. 6) give two relationships analogously to (1) and (2)

$$V_1(l,\theta)=C\int(\sigma_z-\sigma_{x'})\,dy', \tag{30}$$

$$V_2(l,\theta)=2C\int\tau_{zx'}\,dy'. \tag{31}$$

V. A. Sharafutdinov has shown [9] that if experimental data (30) and (31) are recorded in two adjacent sections Δz apart, it is possible to determine the distribution of $\partial\sigma_z/\partial z$ in the section xy. Starting with a plane $z=z_0$ where distribution of σ_z is known, it is possible to recursively determine the distribution of σ_z in the whole model.

However, recursive determination of σ_z is sensitive to experimental errors.

Let us show that it is possible to determine the distribution of σ_z independently in an arbitrary section $z=$const [10].

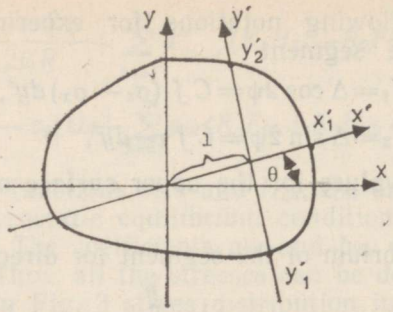

Fig. 6. Investigation of a cross-section of an arbitrary three-dimensional body.

Considering the equilibrium condition in the direction x' of the three-dimensional segment $y'_1 y'_2 x'_1$ (Fig. 6) of thickness Δz we obtain analogously to Eq. (29)

$$\int_{y'_1}^{y'_2} \sigma_z \, dy' = \frac{1}{2C\Delta z}\left(\int_{l}^{x'_1} V'_2 \, dx' - \int_{l}^{x'_1} V_2 \, dx'\right) - \frac{V_1}{C} + \frac{P_{x'}}{\Delta z}, \qquad (32)$$

where $P_{x'}$ is the external load in the direction of x' at the external surface $y'_1 x'_1 y'_2$ of the segment.

Since relationships (32) can be obtained for all rays with parameters 1 and θ, the determination of σ_z is reduced to a problem of scalar field tomography.

As an example, Fig. 7 shows the distribution of axial residual stress in a cylindrical fibre preform with elliptical core and cladding.

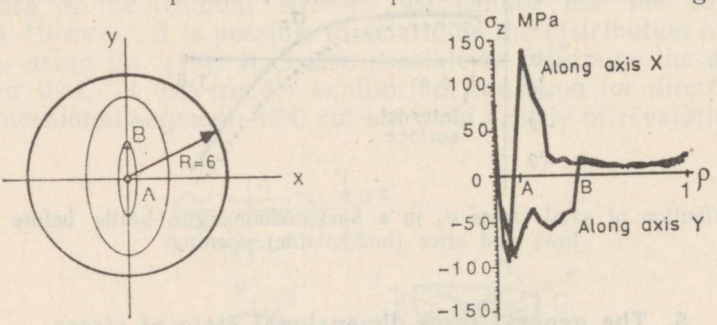

Fig. 7. Cross-section of a fibre preform and axial stress distribution along axes x and y.

If external loads meet certain restrictions (absence of twist), the distribution of σ_z permits to calculate also the values of other components of the stress tensor.

6. Conclusions

It has been shown that in case of weak birefringence the measurements and theory of integrated photoelasticity are considerably simpler and it is possible, with some restrictions, to determine also the general three-dimensional state of stress.

Birefringence is often weak in glass specimens, in models made of plexiglass, in specimens of NaCl and KCl, etc. One may also use models of optically sensitive materials like epoxy resin. However, in the latter case the model should be free of initial birefringence and the load should be kept low.

REFERENCES

1. *Aben, H.* Integrated Photoelasticity. New York, McGraw-Hill, 1979.
2. *Herman, G. T.* Image Reconstruction from Projections. New York, Academic Press, 1980.
3. *Aben, H. K.* // Proc. Internat. Symp. Photoelasticity (Tokyo, 1986). Tokyo, Springer, 1986, 243—250.
4. *Aben, H.* // Rev. franç. méc., 1989, № 1, 121—130.
5. *Aben. H. K., Josepson, J. I., Kell, K.-J. E.* // Opt. and Lasers in Engineering, 1989, **11**, № 3, 145—157.
6. *Davin, M.* // C. R. Acad. Sci. Paris, 1969, **A 269**, № 12, 473—476.
7. *Doyle, J. F., Danyluk, H. T.* // Exp. Mech., 1987, **18**, № 6, 215—220.
8. *Neuber, H.* Kerbspannungslehre. Berlin, Springer, 1985.
9. *Шарафутдинов В. А.* // Тез. докл. IV Всесоюзн. семинара по вычислительной томографии (Ташкент, 1989). Новосибирск, 1989, **1**, 50—51.
10. *Пуро А. Э.* // Тез. докл. IV Всесоюзн. семинара по вычислительной томографии (Ташкент, 1989). Новосибирск, 1989, 1, 36—37.

Estonian Academy of Sciences,
Institute of Cybernetics

Received
Feb. 27, 1990

Hillar ABEN, Siim IDNURM, Alfred PURO

INTEGRAALNE FOTOELASTSUS NÕRGA KAKSIKMURDVUSE KORRAL

Peapingete suundade pöördumise tõttu on integraalses fotoelastsuses optilised nähtused keerukad ning pöördülesande lahendamisel tuleb kasutada mittelineaarseid seoseid pingevälja parameetrite ja katseandmete vahel. On näidatud, et nõrga kaksikmurdvuse korral lihtsustuvad oluliselt optilised mõõtmised ning katseandmed avalduvad pingetensori komponentide integraalidena. See võimaldab välja töötada meetodeid ruumilise pingevälja mittepurustavaks määramiseks läbipaistvates katsekehades.

Хиллар АБЕН, Сийм ИДНУРМ, Альфред ПУРО

ИНТЕГРАЛЬНАЯ ФОТОУПРУГОСТЬ В СЛУЧАЕ СЛАБОГО ДВУПРЕЛОМЛЕНИЯ

Вследствие вращения направлений главных напряжений оптические явления в интегральной фотоупругости являются сложными, а решение обратной задачи базируется на нелинейных соотношениях. Показано, что в случае слабого двупреломления оптические измерения значительно упрощаются и данные измерения выражаются интегралами от компонентов тензора напряжения. Это позволяет выработать методы для неразрушающего определения трехмерного поля напряжений в прозрачных телах.